

# A COMPARATIVE STUDY OF PHOTOCONDUCTIVITY DECAY IN ZnO-BASED MSM STRUCTURES AND NANOWIRES

E. Rusu<sup>1</sup>, V. Postolache<sup>2</sup>, N. Curmei<sup>1</sup> and V. Ursaki<sup>1</sup>

<sup>1</sup>*Institute of Electronic Engineering and Nanotechnologies “D. Ghițu”,  
Academy of Sciences of Moldova, Academiei str. 3, Chisinau, MD-2028 Republic of Moldova  
E-mail: rusue@nano.asm.md*

<sup>2</sup>*National Center for Materials Study and Testing, Technical University of Moldova,  
bd. Stefan cel Mare 168, Chisinau, MD-2004 Republic of Moldova*

(Received September 20, 2016)

## Abstract

Comparative analysis of transient photoconductivity in ZnO-based MSM structures and nanowires is performed in this paper. The measurements are carried out at room temperature in ambient air. The mechanisms of photoconductivity decay are discussed taking into account the range of measured relaxation times. It is found that the photoconductivity decay is determined by bulk effects in MSM structures, while it is governed by surface states and surface band bending effects in networks of nanowires.

## 1. Introduction

The relaxation processes of photoconductivity (PC), especially the effects related to long-duration PC decay and persistent photoconductivity (PPC) can significantly affect the parameters of photodetectors, field effect transistors, gas sensors, and other devices in terms of their sensitivity, noise properties, dark level, and temporal characteristics. PPC effects can be caused by various factors, particularly defects with bistable character, such as DX [1, 2] or AX centers [3], microscopic inhomogeneity [4, 5], and other effects leading to the formation of potential barriers induced by random local potential fluctuations.

It is generally believed that the mechanism of PPC in moderately doped bulk semiconductors, such as III–V alloys, is due to the metastable behavior of DX centers with a large lattice relaxation following electron capture by the DX state.

The spatial separation of the photogenerated electrons and holes by macroscopic potential barriers can occur due to band bending around doping inhomogeneities, or at planar surfaces, interfaces, junctions, etc. Particularly, a microscopic inhomogeneity caused by impurity distribution is produced in highly doped compensated semiconductors. The mechanism with macroscopic potential barriers is also inherent in II–VI semiconductor alloys. In this case, the random local potential fluctuations are caused by compositional fluctuations.

It has been speculated that, in nanowires, for instance, in ZnO nanowires, PPC is caused by a strong surface band bending (SBB) effect instead of a bulk trap effect [6, 7]. ZnO has been shown to be a versatile material for sensor applications, particularly for a visible-blind ultraviolet (UV) sensor [8] suitable for both military and non-military applications [9]. ZnO nanowire-based photodetectors and optical switches are of particular interest [10, 11].

The goal of this paper is to perform a comparative study of PC decay in ZnO-based metal–semiconductor–metal (MSM) structures and nanowires and identify the mechanism of PC relaxation processes.

## 2. Sample preparation technique

To prepare MSM structures, ZnO films were deposited on *p*-type Si substrates by the spin-coating method. A chemical solution was prepared for these purposes by dissolving zinc acetate dihydrate  $[\text{Zn}(\text{CH}_3\text{COO})_2 \cdot \text{H}_2\text{O}]$  in 2-methoxyethanol at room temperature. Diethanolamine (DEA) was added to the initial mixture as a stabilizer. A solution composed of  $\text{InCl}_3$  in 2-methoxyethanol was used for doping. The final mixture was subjected to ultrasound treatment at  $50^\circ\text{C}$  during 1 h until total homogenization.

The design of MSM optical sensors was produced by photolithography. The film was covered with a positive AZ5214E photoresist by spin coating and then exposed to radiation from a 250-W mercury lamp through masks for 60 s. In regions for metallic contacts, dissolution was performed in a NaOH solution with a concentration of 1% for 4 s.

Figure 1 shows the sequence of procedures for the production of MSM structures, including the deposition of a ZnO film on a Si substrate (Fig. 1a), a photoresist layer (Fig. 1b), the exposure of the photoresist through the mask with a required design (Fig. 1c), and the metallization of regions for electrical contacts in the inter-digital design of the device (Fig. 1d). Aluminum ohmic contacts were deposited on the surface of the ZnO layer by means of thermal vaporization in vacuum. The sample was heated to  $100^\circ\text{C}$  during metal deposition to improve the adhesion. The Al contacts were heated to  $250^\circ\text{C}$  for 30 min after removing the photoresist.

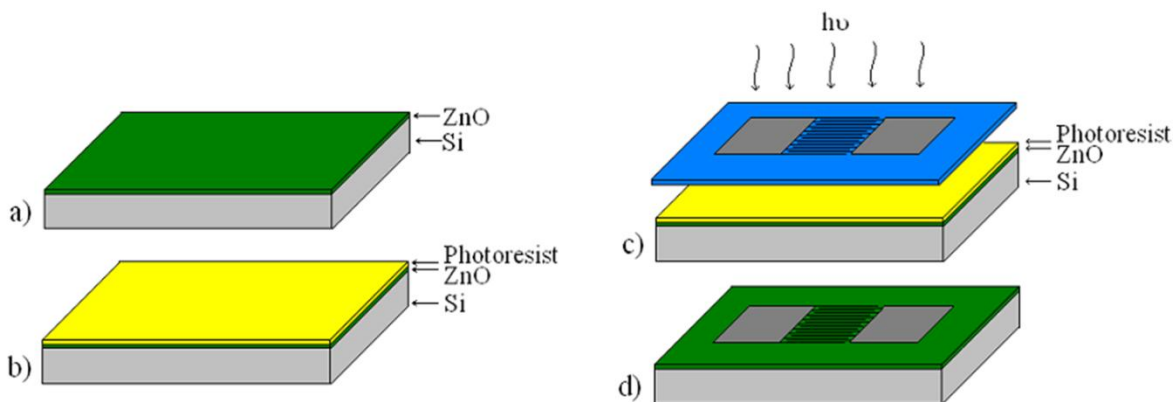


**Fig. 1.** Sequence of procedures for the production of MSM structures.

ZnO nanowires were prepared in a two-step technological route on the basis of Na-doped bulk ZnTe single crystals with a free hole concentration of  $3 \times 10^{18} \text{ cm}^{-3}$ . A template of ZnTe nanowires with a mean diameter around 50 nm was produced in the first step by electrochemical treatment of ZnTe crystals as described elsewhere [12]. Anodic etching was conducted in an  $\text{HNO}_3 : \text{HCl} : \text{H}_2\text{O}$  electrolyte at a ratio of 5 : 20 : 100 at  $25^\circ\text{C}$  with the application of 0.3-s voltage pulses at a frequency of 1 Hz and an amplitude of 5 V. The ZnTe nanowires were

transformed into ZnO nanowires in the second step by thermal treatment. The morphology of the nanowires did not change during annealing at 500°C, while the material was totally oxidized. Morphological and chemical composition microanalyses of the samples were conducted using a VEGA TESCAN TS 5130MM scanning electron microscope equipped with an Oxford Instruments INCA energy dispersive X-ray system. Figure 2 shows the design of the MSM structure and the morphology of the produced ZnO nanowires.

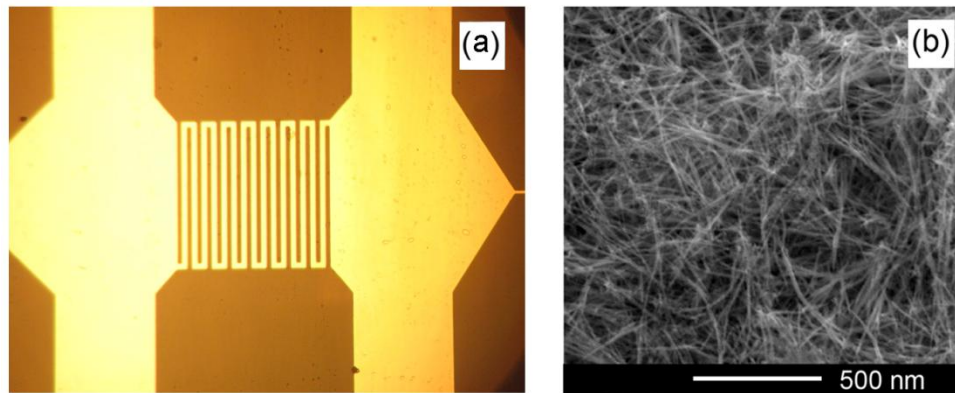


**Fig. 2.** Design of the MSM structure (a) and morphology of the produced ZnO nanowires (b).

### 3. PC relaxation in MSM structures and ZnO nanowires

The electrical contacts to samples for measuring PC were prepared using a conductive silver paste. Since the decay time is fairly long in a network of ZnO nanowires, a 366-nm excitation beam of an Hg arc lamp was mechanically shut in the PC relaxation experiments. The experiments were performed at room temperature in ambient air.

The current–voltage characteristics of the MSM structure exhibit an ohmic behavior (Fig. 3), which indicates that the contacts will have no effect on the current relaxation processes in MSM structures, the PC decay being related entirely to the bulk of the ZnO film.

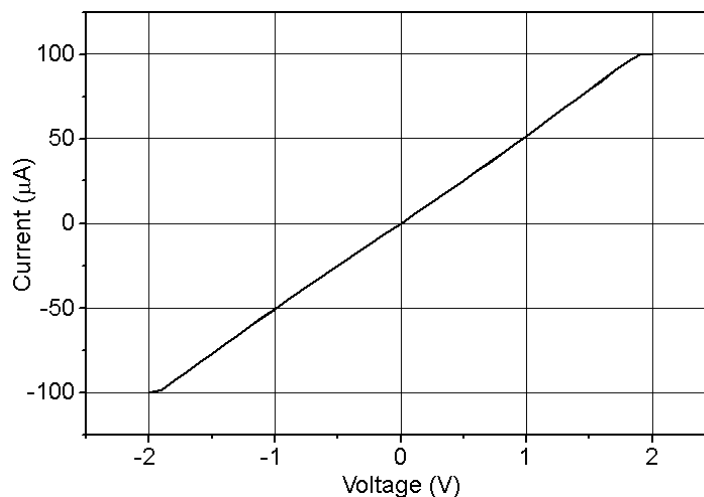


**Fig. 3.** Current–voltage characteristic of an MSM structure.

The PC decay in MSM structures is fairly fast (Fig. 4a); this feature indicates the predominance of bulk mechanisms, while the PC relaxation processes in nanowire samples have a different nature (Fig. 4b). First of all, the relaxation time is much longer than that for the SMS sample. This large relaxation time cannot be attributed to trapping effects of bulk centers. Models with microscopic (atomic) energy barriers at centers with large lattice relaxation, such as DX centers, have not been reported in ZnO either. On the other hand, the SBB effects are generally accepted as the origin for long relaxation times and PPC in ZnO nanowires [11, 13]. The fact that the shape of the relaxation curves in ZnO nanowires is not affected by a change in the applied bias and the polarity of the bias indicate that, similarly to MSM structures, there is no influence of contact effects.

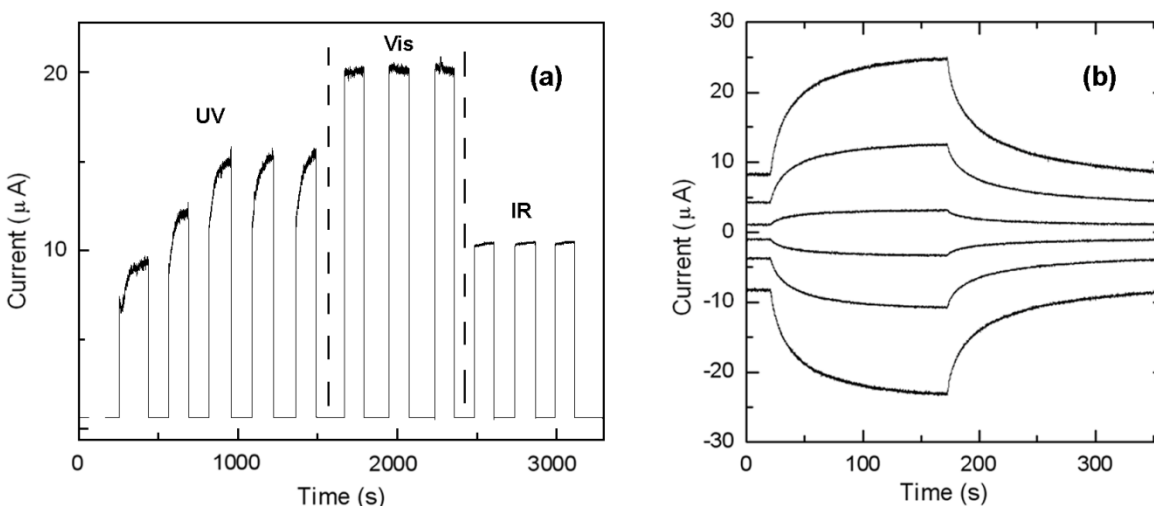


**Fig. 4.** PC build-up and decay measured at room temperature in a MSM photoconductor with excitation from different spectral ranges (a) and in ZnO nanowires (b) with UV radiation power density of  $250 \text{ mW/cm}^2$  at different applied biases (from top to bottom, the curves were recorded at an applied external bias of 5, 3, 1, -1, -3, and -5 V, respectively).

Typically, wide bandgap metal oxide semiconductor nanostructures exhibit current sensitivity only in UV region [14, 15]. However, photodetection in a wide spectral range is of interest for many applications. The current switching behavior in Fig. 4a shows that the MSM structures exhibit strong photosensitivity in a wide spectral range from the UV to infrared (IR) wavelengths. ZnO nanomaterials typically exhibit photodetection in the range from UV to visible region. On the other hand, the prepared MSM structures show a switching behavior in the infrared region too. Therefore, they have a potential to be utilized as universal photodetector devices in contrast to common devices based on wide bandgap semiconductors. The fact that, in the prepared MSM samples, PC is induced not only by UV irradiation, but also by visible and near-infrared light irradiation can suggest the presence of a large amount of energy levels within the bandgap of ZnO films, and these energy levels can also form extended band-edge tails of the density of states, which generate electron-hole pairs by radiation with a large spectrum of wavelengths.

As concerns the ZnO nanowires, they are randomly oriented and the percolation, as deduced from Fig. 2b, provides a pathway of current through the nanowire network. The mechanisms of photoresponse in ZnO nanowires are commonly attributed to their huge surface-

to-volume ratio and to surface effects related to adsorption (in the dark) and desorption (under UV illumination) of oxygen molecules when measurements are performed in ambient air [16]. The adsorption of oxygen molecules to the ZnO nanowire surface in the dark results in capture of free electrons of the *n*-type semiconductor:  $O_2(g) + e^- \rightarrow O_2^-(ad)$ , which produces a depletion layer near the nanowire surface and upward band bending near the surface. The adsorption of oxygen molecules significantly reduces the conductivity of the nanowires due to the large surface-to-volume ratio. Electron-hole pairs are generated in ZnO under UV-light illumination with photon energy higher than the bandgap. Consequently, the holes migrate to the surface along the potential slope created by the band bending and recombine with  $O_2^-$ -trapped electrons. As a result of this recombination, oxygen is released from the surface according to the reaction  $O_2^-(ad) + h^+ \rightarrow O_2(g)$ . On the other hand, the unpaired electrons contribute to the PC.

#### 4. Conclusions

The results of this comparative study have shown different mechanisms of PC relaxation in ZnO-based MSM structures and nanowires. The PC relaxation is fairly fast in MSM structures, being determined by bulk effects in ZnO films. In ZnO nanowires, the PC relaxation is governed by surface effects, such as adsorption and desorption of oxygen molecules, SBB effect, recombination of photogenerated holes with electrons trapped at oxygen molecules, and contribution of photogenerated electrons to PC, which results in longer relaxation times and PPC. The spectral distribution of PC is also different in ZnO-based MSM structures and nanowires. In nanowires, PC is generated predominantly by the above bandgap radiation, while in MSM structures it is generated in a wider spectral range from UV to IR wavelengths, suggesting the presence of a large amount of energy levels within the bandgap of ZnO films which can also form extended band-edge tails of the density of states. Due to the wide spectral range of PC in ZnO-based MSM structures, they have a potential to be utilized as universal photodetector devices.

#### References

- [1] D. V. Lang, R. A. Logan, and M. Jaros, Phys. Rev. B 19, 1015, (1979).
- [2] J. Z. Li, J. Y. Lin, H. X. Jiang, M. A. Khan, and Q. Chen, J. Appl. Phys. 82, 1227, (1997).
- [3] J. Z. Li, J. Y. Lin, H. X. Jiang, A. Salvador, A. Botchkarev, and H. Morkoc, Appl. Phys. Lett 69, 1474, (1996).
- [4] H. J. Queisser, and D. E. Theodorou, Phys. Rev. B 33, 4027, (1986).
- [5] H. X. Jiang, G. Brown, and J. Y. Lin, J. Appl. Phys. 69, 6701, (1991).
- [6] H.-Y. Chen, R.-S. Chen, N. K. Rajan, F.-C. Chang, L.-C. Chen, K.-H. Chen, Y.-J. Yang, and M. A. Reed, Phys. Rev. B 84, 205443, (2011).
- [7] C. Soci, A. Zhang, B. Xiang, S. A. Dayeh, D. P. R. Aplin, J. Park, X. Y. Bao, Y. H. Lo, and D. Wang, Nano Lett. 7, 1003, (2007).
- [8] G. Goncalves, J. Non-Cryst. Solids 352, 1444, (2006).
- [9] S. Hullavarad, N. Hullavarad, D. Look, and B. Claflin, Nanoscale Res Lett 4, 1421, (2009).
- [10] J. B. K. Law, and J. T. L. Thong, Appl. Phys. Lett 88, 133114, (2006).
- [11] C. Soci, A. Zhang, X.-Y. Bao, H. Kim, Y. Lo, and D. Wang, D., Nanotechnology 10, 1430, 2010.

- [12] V. Zalamai, A. Burlacu, V. Postolache, E. V. Rusu, V. V. Ursaki, and I. M. Tiginyanu, *Mold. J. Phys. Sci.* **9**, 308, (2010).
- [13] D. Cammi, and C. Ronning, *Adv. Cond. Matter Phys.* **2014**, 184120, (2014).
- [14] D. Gedamu, D. et al., *Adv. Mater.* **26**, 1541, (2014).
- [15] H. Chen, L. Hu, X. Fang, and L. Wu, *Adv. Funct. Mater.* **22**, 1229, (2012).
- [16] Y. K. Mishra, Y. K. et al., *ACS Appl. Mater. Interfaces* **7**, 14303, (2015).